J Mater Sci: Mater Med (2011) 22:137–149
DOI 10.1007/s10856-010-4169-3

Evaluation of in situ albumin binding surfaces: a study of protein adsorption and platelet adhesion

Sanjukta Guha Thakurta · Anuradha Subramanian

Received: 1 June 2010 / Accepted: 7 October 2010 / Published online: 1 December 2010

Abstract Surface modification strategies that take advantage of the passivation effects of albumin are important in the development of biomaterial surfaces. In this study, linear peptides (LP1, LP2) and a small chemical ligand (SCL) with albumin binding affinities were grafted onto silane functionalized silicon substrates. Surfaces were characterized with contact angle and ellipsometric measurements, and densities of immobilized ligands were assessed spectroscopically. Ellipsometrically measured thickness correlated with the predicted molecular lengths of grafted moieties. Contact angle analysis indicated that the LP1 and LP2 functionalized surfaces were hydrophilic compared to SCL functionalized and control surfaces. Adsorption of albumin from human serum was evaluated and quantified via specific enzyme-linked immunosorbent assays and 2D gel electrophoresis. The following trend was noted for surface adsorbed albumin: LP1 > LP2 > SCL > C, with LP1 derivatized surfaces having $\sim$2.450 μg/cm^2 of bound albumin. LP1 derivatized surfaces possessed the least number of adsorbed platelets with rounded platelet morphology when compared to control surface.

1 Introduction

Biomaterials that offer improved thrombogenicity and material characteristics can improve material performance in vivo [1–4]. While many factors contribute to the failure and rejection of biomedical implants, surface-induced thrombosis has been reported to play an important role [4]. Even though most biomedical polymers are relatively inert, non-reactive and non-toxic, most implant materials when exposed to physiological fluids are coated with a complex layer of proteins, which in-part initiate surface-induced thrombotic events [4–7]. Previous research has reported that the adsorption pattern of plasma proteins was influenced by the chemical and physical characteristics of a variety of biomaterial surfaces [8–11]. In addition to the adsorption of the key plasma proteins; namely, albumin, immunoglobulin and fibrinogen, the adsorption of Von Willebrand factor (vWF), fibronectin and vitronectin have also been reported [5]. Albumin-coated surfaces adhere fewer platelets whereas γ-globulin and fibrinogen adsorbing surfaces promote the adhesion of platelets [8–15]. Thus, surface modification strategies to yield surface-coated or surface adsorbed albumin have been developed to take advantage of the surface passivation effects of albumin coatings.

Previous research to engineer surfaces with enhanced albumin affinity includes surfaces modified with straight chain 16- or 18-carbon alkyl chains, the modification of PU and PU-PHEMA surfaces with dextran: cibacron blue (CB) dye conjugate, immobilization of albumin specific monoclonal antibodies [16–18]. While previous work has provided useful and critical insights, by highlighting the importance of surface, surface chemistry, spacer moieties, affinity ligands, epitope presentation, and surface interactions in the process of protein adsorption, an opportunity exists to design and develop small chemical ligands or peptides with high selectivity and specificity for albumin binding and a defined surface chemistry to anchor these ligands. Thus, in the present paper, peptide- or small

Electronic supplementary material The online version of this article (doi:10.1007/s10856-010-4169-3) contains supplementary material, which is available to authorized users.

S. Guha Thakurta · A. Subramanian (✉)
Department of Chemical and Biomolecular Engineering, University of Nebraska, Lincoln, NE 68588, USA
e-mail: asubramanian2@unl.edu

chemical ligand derivatized biomaterial surfaces were generated in an attempt to control protein-surface interactions and confer in situ albumin binding properties. Albumin binding peptides that were generated by the phage-display method and characterized elsewhere were used in our studies [19]. Additionally, a small chemical ligand that has been shown to preferentially interact with human serum albumin over other plasma proteins was also employed [20].

The central hypothesis is that surfaces developed in this study will preferentially recruit albumin in situ to keep the surface coated with albumin and result in surfaces with increased albumin binding and lower platelet adhesion when compared to a control surface. In this study, silicon wafers were used as a model substrate and self-assembled monolayers were fabricated using 3-aminopropyltriethoxysilane (APTES) to serve as a template for protein immobilization on silicon surfaces. The silane derivatized surfaces were modified further using three different ligands that have been reported to bind human serum albumin (HSA), namely: linear peptides; a 31-mer (AEGTGDFWFCDRIAWYPQHLCEF LDPEGGGK; denoted as LP1), a 14-mer (DRIAWYPQ HLGGGK; denoted as LP2) and a small synthetic ligand (2, 4, 6-Tris (dimethylaminomethyl) phenol; denoted as SCL) [19, 21]. The protein binding capacity of these surfaces was quantified by specific ELISA (enzyme-linked immunosorbent assay) and by 2D gel electrophoresis. The adhesion of platelets to the modified surfaces was evaluated by scanning electron microscopy and quantified via lactate dehydrogenase assays.

2 Experimental

2.1 Materials

Silicon (100) wafers, p-type, 2 inch diameter, one side polished, resistivity <0.01 were purchased from Polishing Corporation of America (Santa Clara, CA). Unless otherwise stated, all chemicals were ACS grade or better, and used as received. 3-aminopropyltriethoxysilane (APTES) was obtained from Gelest, Inc. (Morrisville, PA). Peptides: namely LP1 (AEGTGDFWFCDRIAWYPQHLCEFLDPEGGGK) and LP2 (DRIAWYPQHLGGGK) were custom made from Sigma-Genosys (Spring, TX). 1-Ethyl-3-[3-dimethylaminopropyl] carbodiimide hydrochloride (EDC) and N-hydroxysulfosuccinimide (NHSS) were obtained from Pierce (Rockford, IL) and were used to crosslink peptides to surface. 2,4,6-Tris(dimethylaminomethyl)phenol (technical, ≥90%, NT) was the small chemical ligand (SCL) and the 1,4-butanediyl diglycidyl ether (technical grade, 60%) was respective cross linker which were obtained from Sigma (St. Louis, MO). A Teflon beaker was used for hydrofluoric acid treatments. All the rinsing steps involved in the experiments utilized deionized water with resistivity 18 MΩ cm.

2.1.1 Serum proteins and antibodies

Human serum albumin (A9511), rabbit anti-human IgG antibody whole molecule (I2011), HRP conjugated rabbit anti-human IgG (A8792), human serum fibrinogen (F4129), QuantiPro™ BCA assay kit (QPBCA), In Vitro Toxicology Assay Kit: Lactic Dehydrogenase based, SIGMAFAST™ OPD tablets, dialysis tubing cellulose membrane (MWCO 12400) were purchased from Sigma (St. Louis, MO). Human immunoglobulin G (HGG5000) and human serum were obtained from EquitechBio. Inc. (Kerrville, TX). Affinity purified goat anti-human albumin antibody (A80129A) and HRP conjugated goat anti-human albumin antibody (A80129P) were obtained from Bethyl Laboratories, Inc. (Montgomery, TX). Polyclonal rabbit anti-human fibrinogen antibody (A0080), HRP conjugated rabbit anti-human fibrinogen antibody (A8792) were purchased from Dako Cytomation (Carpinteria, CA). SDS-OUT™ SDS precipitation kit and Silver snap stains were obtained from Thermo scientific (Chicago, IL). The complete ZOOM® Bench top Proteomics System, 4X NuPAGE® LDS sample buffer, NuPAGE® sample reducing agent, NuPAGE® antioxidant, MOPS running buffer, Mark12™ unstained standard molecular ladder were obtained from Invitrogen (Carlsbad, CA) for 2D Gel electrophoresis. Bovine blood was collected in acid–citrate–dextrose (ACD) from Veterinary & Biomedical Sciences, University of Nebraska Lincoln (Lincoln, NE).

2.1.2 Buffers

MES buffer (100 mM MES, 500 mM NaCl, pH 6.0) was used to anchor peptides. Phosphate buffer (10 mM Na_2HPO_4, 20 mM NaCl, pH 6.2) was used as exchange buffer (EB) for dialyzing human serum. The exchange buffer without salt (10 mM Na_2HPO_4, pH 6.2) was used as sample incubation buffer (IB) when indicated. Prepared surfaces were stored in 1× phosphate buffer saline (PBS) with 0.01% NaN_3 until use. For human serum albumin (HSA) ELISA, coating buffer (0.05 M carbonate–bicarbonate, pH 9.6), washing buffer (50 mM Tris, 0.14 M NaCl, 0.05% Tween 20, pH 8.0), blocking buffer (50 mM Tris, 0.14 M NaCl, 1% BSA, pH 8.0), dilution buffer (50 mM Tris, 0.14 M NaCl, 1% BSA, 0.05% Tween 20, pH 8.0) were prepared according to the manufacturer's protocol (Bethyl Lab). For human immunoglobulin G (HIgG) and human fibrinogen (HFib) ELISA, coating buffer (0.1 M $NaHCO_3$, 0.1 M NaCl, pH 9.3), washing buffer (20 mM Tris–HCl, 50 mM NaCl, 0.05% Tween 20, pH 7.2), blocking/dilution buffer (20 mM Tris–HCl, 50 mM NaCl, 0.5% casein, pH 7.2) were prepared according to procedures developed in our laboratory. Platelet suspension buffer (134 mM NaCl, 12 mM $NaHCO_3$, 2.9 mM KCl, 0.34 mM

Na_2HPO_4, 1.0 mM $MgCl_2$, 1.8 mM $CaCl_2$, 10.0 mM Hepes, 5 mM glucose, 0.3 g/100 ml BSA) was used to re-suspend platelets after separation from blood. BSA and glucose were added in the warmed solution prior to use of platelet suspension buffer (PSB).

2.2 Surface preparation

The overall scheme to derivatize silicon surfaces and the further synthesis of APTES-modified surfaces with the ligands selected in this study is schematically represented in Fig. 1. Hydroxylation of 1 × 1 cm^2 silicon wafers was carried out by first etching with diluted HF for 5 min followed by oxidation with HNO_3–500 ppm HF mixture at 80°C for 15 min [22]. Hydroxylated silicon wafers were then exposed to anhydrous toluene containing 2 vol.% of APTES for 30 min at room temperature under constant stirring and nitrogen purging. Surfaces were then sonicated and rinsed in (1) toluene, (2) toluene–methanol mixtures (1:1 v/v), and (3) methanol sequentially for 2 min each and then dried in nitrogen atmosphere.

2.2.1 *Coupling of peptides to APTES functionalized surfaces*

For the coupling of peptides (Sigma-Genosys; Spring, TX) to APTES-derivatized surfaces, silanized surfaces were first equilibrated in MES buffer for 30 min. Peptides were dissolved in a minimum volume of dimethylsulfoxide (DMSO) and stored on ice. 1-Ethyl-3-(3-dimethylaminopropyl) carbodiimide hydrochloride (EDC) and *N*-hydroxysulfosuccinimide (NHSS) were first dissolved in MES buffer and then the solution was added to DMSO containing peptide. MES buffer was rinsed off from equilibrated surfaces and peptide solution was added on the surfaces. The reaction was allowed to take place for 12 h at 4°C on a shaker (50 rpm). After peptide coupling, surfaces were washed gently with copious amount of MES.

2.2.2 *Coupling of SCL to APTES functionalized surfaces*

For SCL coupling, silanized surfaces were equilibrated with isopropyl alcohol (IPA) for 30 min and, exposed to 1,4-butanediyl diglycidyl ether (BUDGE) dissolved in IPA for 8 h at room temperature with gentle shaking. Upon the completion of the BUDGE incubation step, surfaces were exposed to SCL (SCL: BUDGE at 6:1 molar ratio) for 24 h at room temperature on a shaker. At the end of incubation, surfaces were washed with DI water. Surfaces prepared were stored in PBS buffer containing 0.01% NaN_3 at 4°C until further use.

Untreated wafer (denoted as C) were rinsed in ethanol followed by sonication and rinsing in DI water and stored under similar conditions.

2.3 Surface characterization

2.3.1 *Ellipsometry*

The increase in film thickness at the end of each step shown in Fig. 1 was measured by spectroscopic ellipsometer M2000 V operating in the UV–Visible region at Center for

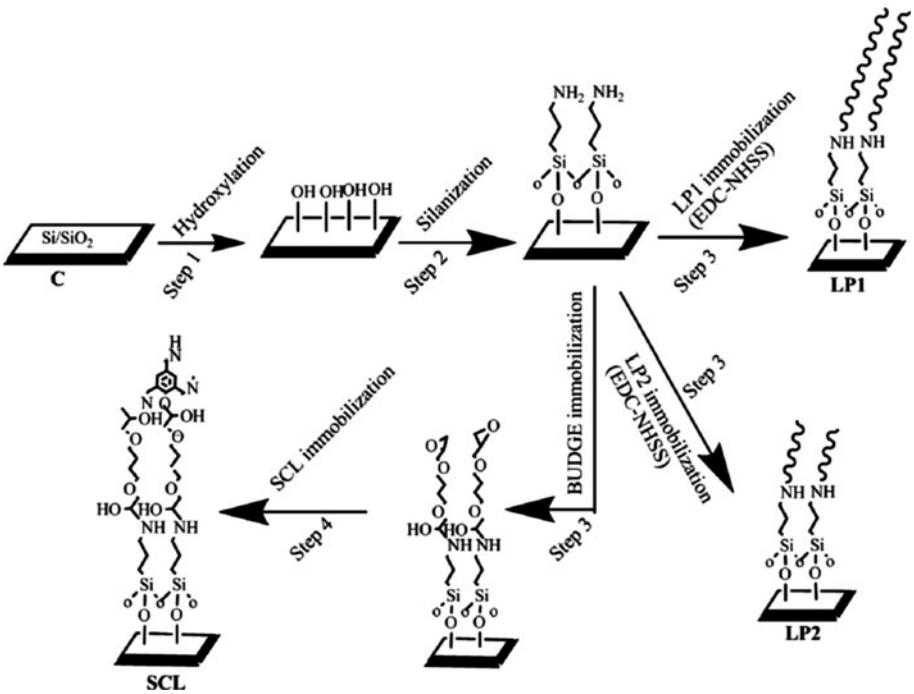

Fig. 1 *Schematic representation of the surface functionalization method.* Silicon wafer was first hydroxylated (step 1) followed by silanization (step 2) with APTES to yield surfaces with –NH_2 moieties. In step 3, linear peptides were covalently anchored to the silanized surface via EDC–NHSS crosslinker. In step-4, SCL was also immobilized on silanized surface (step 4) via a bifunctional epoxide, BUDGE. Unmodified surfaces served as controls (C)

Materials Research and Analysis, University of Nebraska (Lincoln, NE). Spectroscopic ellipsometry measurements were done in air immediately after surface preparation. The experimental data for LP1 and LP2 modified surface were fitted in four-layer models which consist of a silicon base layer and three consecutive uncoupled Cauchy layers. Each Cauchy layer corresponded to different step of surface modification. For SCL anchored surface, the experimental data was fit to five layer models consisting of silicon base layer and four consecutive uncoupled Cauchy layers [23]. Each reported value represented the average value and standard error of at least three separate thickness values from each of the three different batch of experiments ($n = 9$).

2.3.2 UV–Visible spectroscopy

The density of surface grafted peptides (LP1, LP2) and SCL ($n = 6$) were measured with bicinchoninic acid assay and malonic acid–acetic anhydride (MA–AA) condensation assay, respectively [23]. The grafting density of the peptides and SCL immobilized on surfaces was estimated by correlating the concentrations of peptides and SCL in solutions, based on the available amine (BCA assay) and tertiary amine (MA–AA assay) groups, respectively.

2.3.2.1 BCA assay Briefly, three 1×1 cm^2 of peptide grafted (sample) and silanized (blank) surfaces were washed with MES buffer, dried under N_2 atmosphere and placed in well of a six-well TCP plate. Serial dilutions of LPI and LP2 (0–50 μg/ml) served as standard. 1 ml of the QPBCA assay reagent was added per well and incubated at 37°C for 2 h, allowed to cool and absorbance at 570 nm was measured. The average data with standard error was represented here ($n = 6$).

2.3.2.2 MA–AA assay Malonic acid (MA) was pre-desiccated for 24 h at 110°C and was dissolved in acetic anhydride (AA) to make the coloring reagent. Serial dilutions of SCL in tetrahydrofuran (THF) (0–50 μg/ml) were prepared and mixed with coloring reagent at a ratio 1:1.5, allowed to react at room temperature for 20 min and the absorbance at 390 nm was recorded [24]. Three 1×1 cm^2 of SCL grafted (sample) and BUDGE grafted (blank) surfaces were washed with DI water, dried under N_2 atmosphere and placed in well of a six-well TCP plate and 1 ml of coloring reagent was added. After incubation at 50°C for 20 min, absorbance at 390 nm was recorded. The average data with standard error was represented here ($n = 6$).

2.3.3 Contact angle measurement

Advancing contact angle measurement was performed following sessile drop method with OCA 15, SCA 20, Data Physics Instrument GmbH (Filderstadt, Germany). Contact angles (θ) were measured using two polar liquids, DI water, ethylene glycol and two apolar liquids, diiodomethane, α-bromonaphthalene. The size and volume of the drops were kept constant (1 μl with flow rate of 0.1 μl/s). Contact angle measurements were done after an average 6 h of surface preparation. To avoid spreading of the drops and droplet shape variation, contact angle values were recorded within 15–20 s after placing the drop. The average contact angle values were collected from at least five drops on different areas of a modified wafer. Repeated measurements from three different batches of reactions showed all average contact angles values with ±5° standard error. All measurements were conducted in air and at a temperature of 23°C. The method of estimation of polar, apolar component of the surface tension was described elsewhere [22, 25, 26].

2.3.4 Protein adsorption study

2.3.4.1 Protein incubation In separate experiments, surface were incubated with (a) single component protein system (1 mg/ml HSA in IB), and (b) human serum that was dialyzed against exchange buffer [19]. Human serum was dialyzed to render it compatible with the protein incubation and binding conditions. Before incubation, surfaces were copiously washed to remove NaN_3 and placed in wells of a six well TCP plate (three 1×1 cm^2 surfaces/well). Upon incubation for 6 h surfaces were copiously washed, transferred to new TCP plates and surface adsorbed proteins were eluted with 1% SDS [27, 28]. As higher concentration of SDS (2–4%) or CHAPS was noted to inhibit ELISA assays (data not shown) and interfere with routine sample concentration steps, 1% SDS was used to elute proteins. Further, the total amount of proteins eluted were noted to be similar between CHAPS and 1% SDS treatments [23]. The total protein was quantified using microplate BCA assay as per manufacturer's instructions. The protein samples were stored in aliquots at −20°C until further analysis. Eluates obtained from surfaces exposed to human serum were further analyzed with two dimensional gel electrophoresis and ELISA.

2.3.4.2 Two dimensional gel electrophoresis The 1% SDS eluates samples were treated with SDS-Out™ precipitation kit before running the 2D gels according to manufacturer's protocol. The samples were then rehydrated by mixing with 8 M Urea, 2% CHAPS, 0.5% (v/v) ZOOM® Carrier Ampholytes, 0.002% Bromophenol Blue, and 20 mM DTT (Invitrogen; Carlsbad, CA) and a total protein of 2 μg was loaded onto immobilized pH gradient (IPG, linear gradient, pH range 3–10) gel strips. The feed human serum was also analyzed with 2D gel and 20 μg of

total protein were loaded. 2D gel electrophoresis and staining were carried out according to the manufacturer's protocol. Digital images of the gels were analyzed using DECODON Delta2D software, DECODON GmbH (Greifswald, Germany). Protein spot identification was obtained by matching the gel with the plasma master gel from the Swiss-2DPAGE database (http://www.expasy.org).

2.3.4.3 ELISA The concentration of HSA, HIgG and HFib in various samples was determined by the ELISA procedure outlined elsewhere [29, 30]. Briefly, the plates coated with goat anti-human albumin antibody, rabbit anti-human IgG antibody or rabbit anti-human fibrinogen antibody for HSA, HIgG and HFib ELISA, respectively. Protein standard curves were prepared in both sample buffer and buffer containing 1% SDS and eluate samples were diluted in sample buffer. Bound HSA, HIgG and HFib were detected with HRP conjugated goat anti-human albumin antibody, rabbit anti-human IgG antibody or rabbit anti-human fibrinogen antibody, respectively. A SIGMA-FAST™ OPD tablet was used as substrate. The bound chromophores were recorded at 490 nm with an ELX 800 absorbance microplate reader, BioTek Instruments (Winooski, VT). All samples were assayed in triplicates of quadruplicate applications.

2.4 Platelet adhesion study

2.4.1 Washed platelet preparation

Bovine blood in acid-citrate-dextrose (ACD) was subjected to centrifugation at $200\times g$ for 20 min at room temperature. Platelet rich plasma (PRP) was pipetted out and PRP was subjected to an additional step of centrifugation. PRP was centrifuged at $2{,}000\times g$ for 12 min at room temperature and the clear, pale yellow supernatant was discarded. Platelet precipitate was re-suspended gently in PSB to make washed platelets and the concentration was measured with an Advia 2120 Multispecies Hematology Analyzer at Physicians Laboratory Services (Lincoln, NE). The surfaces were tested with washed platelets within 4 h of platelet preparation.

2.4.2 Surface-washed platelet incubation

Surfaces were first directly exposed to human serum, washed copiously and hydrated with PSB buffer for at least 3 h at 37°C in TCP plates. Collagen coated cover slide (positive control) were also hydrated with PSB buffer. The platelet concentration for adhesion studies was adjusted to be $\sim 1 \times 10^8$/ml of PSB and added to the test surfaces after aspirating the buffers and incubated for 1 h at 37°C under static conditions. After 1 h, the platelet suspension was removed and the surfaces were quickly rinsed with PSB before proceeding with the characterization steps.

2.4.3 Lactate dehydrogenase assay (LDH assay)

Several dilutions were made from the stock platelet suspensions with PSB, and LDH assay analysis was undertaken according to manufacturer's protocol to make a standard curve. The calibration curve was made of LDH activity versus platelet number based on the Hematology Analyzer measurement of the original stock platelet suspension in cells per milliliters.

At the completion of the incubation step of test surfaces with platelets, the surfaces were washed with PSB briefly, transferred to a new TCP plate and 1/10th volume of commercially available lysis buffer (100 µl for 1 cm^2 surface) was added to release the platelets. The concentration of the platelets was measured as detailed earlier and the calibration curve was used to quantify the number of adhered platelets.

2.5 Scanning electron microscopy (SEM) analysis

The morphology of surface adhered platelets was analyzed by SEM analyses. Test surfaces that were exposed to platelet suspensions were gently rinsed with PSB, fixed with 2% glutaraldehyde for 1 h, sequentially dehydrated with ethanol solutions and finally dried overnight [31–33]. All surfaces were sputter-coated with gold and examined using a Hitachi S4700 Field-Emission SEM at Center of Biotechnology, University of Nebraska Lincoln (Lincoln, NE).

2.6 Statistical analysis

In general, the quantitative results and bar graphs were expressed as the mean value ± standard error (SE) over the sample number n. Any significant differences were measured using two sample t-tests assuming unequal variance and $P < 0.005$ was considered statistically significant.

3 Results

The ligand-derivatized surfaces were characterized by ellipsometry, contact angle analysis. The amount of surface immobilized ligand was determined by UV–Visible spectroscopic analysis and the respective values are reported in Tables 1 (ellipsometry and UV–Visible spectroscopy) and 2 (contact angle). The thickness obtained after hydroxylation (step 1) was 2.484 ± 0.106 nm which included –OH-terminated silicon oxides in addition to the bare

unmodified silicon wafer. The thickness obtained after silanization (step 2) was 1.103 ± 0.219 nm, where a theoretical monolayer of APTES was calculated to be 0.916 nm. After the EDC-NHSS step, no thickness increase was observed on silanized surfaces; however, an increment of 1.626 ± 0.313 nm was noticed after anchoring BUDGE (step 3 of SCL). Table 1 shows the increase in thickness upon the covalent immobilization of the LP1 and LP2 on –NH_2-functionalized silicon surfaces and SCL on BUDGE-functionalized surface as measured by VASE and modeled by Cauchy layer approximation. The calculated theoretical length of the LP1, LP2, and SCL moiety under fully stretched condition were 4.557, 2.058, and 0.718 nm, respectively. The resultant thickness upon the covalent immobilization of selected ligands listed in Table 1 match the calculated values.

The immobilization methods for LP1 and LP2 were tailored such that the carboxyl moiety on the peptides reacted with the –NH_2 group of the surface anchored APTES. In the case of SCL, the –OH group on 2,4, 6-tris(dimethylaminomethyl)phenol was reacted with the epoxide group of the grafted BUDGE on surface anchored APTES. The presence of these groups were assayed and reported as surface densities (μmol/cm^2) in Table 1. A 2-fold higher surface density of immobilized LP2 was obtained as compared to LP1. Peptide- or SCL-immobilized surfaces were also characterized by AFM (supplementary Figure 1) and surfaces with low roughness ($R < 1$ nm) were obtained.

The measured contact angles on LP1, LP2, SCL, C surfaces with polar and apolar liquids and the corresponding surface components as estimated using the equations listed in previous literature [25, 26] are shown in Table 2. The contact angle measurement with the polar liquids showed a slight increase in the measured value for surfaces functionalized with LP2 (42.1 ± 1.0) when compared to surfaces functionalized with LP1 (36.5 ± 0.5). However, the increase was more noticeable for surfaces functionalized with SCL surface (57.3 ± 0.4), indicating an increase in the hydrophobic nature of the surface. A contact angle of 85.1 ± 0.6 was noted for C indicating a highly hydrophobic surface. The variation in the apolar component of surface tension was similar to the observed trend with contact angle measurements. The following trend was noted for the negative polar component of surface tension of functionalized surfaces: LP1 > LP2 > SCL > C. The variation in the positive polar component of surface tension was indiscernible. Our results indicate that peptide-terminated surfaces were more hydrophilic compared to SCL-functionalized and C surface. No noticeable change in the computed values of the surface free energy was observed. The interfacial surface free energy (mJ/m^2), which is an indirect measure of the net hydrophilicity of a surface, was observed to vary with ligands used to functionalize APTES modified surfaces (Table 2). Values of −25.998 ± 2.326, 26.387 ± 1.402, and 46.305 ± 1.727 mJ/m^2 were noted for LP1, SCL functionalized and C surfaces, respectively. A change in polarity was observed between LP1-, LP2- and SCL-modified surfaces.

The amount of total protein in the eluate fractions, obtained upon the exposure of test surfaces to either (a) pure HSA or (b) human serum were estimated with BCA assay and ELISA, respectively, and reported in Table 3. The levels of HSA (∼4.5 mg/ml), HIgG (∼1.5 mg/ml) and HFib (0.3 mg/ml) in the human serum feed sample were also confirmed by specific ELISA assays (Table 3). Typically three 1 × 1 cm^2 surfaces were exposed to 1 ml of serum, thus equaling an exposure of ∼ 4.5 mg of HSA, ∼1.5 mg of HIgG, and ∼0.3 mg of HFib, respectively (based on levels estimated by ELISA, Table 3). Though the level of fibrinogen in serum is lower compared to levels reported in plasma (2.0–4.5 mg/ml), the individual protein exposures employed in this paper are comparable to the amounts reported in previous studies that use 1/10th diluted plasma [34, 35]. Surfaces derivatized with LP1 were noted to adsorb 5-fold higher amounts of surface adsorbed HSA/cm^2 when compared to C. The total amount of adsorbed HSA on C and surfaces derivatized with LP2 or SCL was

Table 1 Surface characterization

	UV–Visible spectroscopy	Ellipsometry	
Surface	Ligand packing density (μmol/cm^2)	Theoretical length (nm)	Measured thickness (nm)
LP1	0.069 ± 0.017*	4.557	4.146 ± 0.179
LP2	0.152 ± 0.027*	2.058	1.547 ± 0.130
SCL	0.287 ± 0.058**	0.718	0.669 ± 0.129
C	–	–	–

The surface density of immobilized ligands was evaluated with BCA (*) and MA–AA (**) assay and the average data with standard error has been reported here ($n = 6$). The increase in thickness upon the completion of steps detailed in Fig. 1 was measured by ellipsometry. Theoretical length was calculated from bond length under fully stretched condition. The reported average and standard error includes $n = 9$ for LP1, LP2, and $n = 3$ for SCL surfaces

Table 2 Contact angle analyses

Surface	Contact angle (θ)				Surface energy (mJ/m^2)				
	DI water	Ethylene glycol	Diiodo methane	α-Bromonaphthalene	Apolar component (γ_s^{LW})	Negative polar component (γ_s^-)	Total polar component ($\gamma_s^{\pm}$)	Surface tension (γ_s)	Interfacial surface tension (γ_{sw})
LP1	36.5 ± 0.5	30.7 ± 0.5	44.6 ± 0.5	57.0 ± 0.4	26.499 ± 0.192	66.646 ± 3.893	13.067 ± 0.523	39.566 ± 0.595	−25.998 ± 2.326
LP2	42.4 ± 1.0	37.5 ± 0.5	44.7 ± 0.7	53.6 ± 0.8	28.157 ± 0.404	45.456 ± 2.441	9.978 ± 0.312	38.136 ± 0.303	−14.034 ± 1.625
SCL	57.3 ± 0.4	47.0 ± 1.1	42.9 ± 0.2	38.7 ± 0.5	35.177 ± 0.221	4.916 ± 00.906	3.009 ± 00.136	38.186 ± 0.246	26.387 ± 1.402
C	85.1 ± 0.6	64.0 ± 0.8	38.2 ± 0.6	24.9 ± 0.5	40.360 ± 0.159	0.252 ± 00.022	0.341 ± 00.166	40.702 ± 0.176	46.305 ± 1.727

The contact angles, measured with DI water, ethylene glycol, diiodomethane, and α-bromonaphthalene surfaces, as indicated are presented. Averages and standard error are reported for $n = 15$

observed to be 2.0 to 2.6-fold lower when compared to LP1 derivatized surfaces. Our results indicate that similar amounts of HIgG were adsorbed on C and surfaces derivatized with LP2 or SCL. Surprisingly, no surface adsorbed HFib was detected in the eluates fractions from surfaces derivatized with LP1 or LP2, where the sensitivity of the HFib ELISA was between 0.3 and 5 ng. Surfaces derivatized with SCL and C yielded 210 and 98 ng/cm^2 of surface absorbed HFib, respectively. The analysis of eluates by both ELISA assays and 2D gel electrophoresis indicates that under the conditions employed, surfaces derivatized with LP1 preferentially adsorb HSA when compared to other plasma proteins. In a separate experiment, surfaces were pre-exposed to pure HSA, followed by copious washing and the exposure to human serum yielding higher values of surface adsorbed HSA/cm^2, lower amounts of surface adsorbed HIgG and undetectable amount of HFib (data not shown). The results summarized here indicate that the surface adsorbed HSA was not replaced by serum proteins, in a significant manner.

2D gel electrophoresis was employed to assess the distribution of adsorbed proteins and shown in Fig. 2. A separate gel was also ran with the feed serum to confirm the presence of desired proteins in the feed (supplementary Figure 2). The identities of proteins present in the eluates fractions were confirmed from reference human serum obtained from Expasy SWISS 2D PAGE database. An area at the intersection of isoelectric point (IP) (5.56–5.88) and MW (67–68 kDa) was designated to be HSA. The heavy chain IgG was spotted at the juncture of IP (6.32–7.92), MW (115–100 kDa) and IP (6.15–9.02), MW (55.7–50 kDa) whereas light chain IgG was designated at IP (4.94–8.81), MW (29–22.6 kDa). For fibrinogen, α-chain was designated at IP (6.66–7.40), MW (67–63 kDa), β-chain was designated at IP (6.10–6.55), MW (56–54.8 kDa); γ-chain was designated at IP (5.07–5.62), MW (51.3–44.7 kDa). All the gel images (2A and 2B) were mapped with respect to master human plasma reference gel to identify the spots using DECODON Delta 2D software.

To quantify the relative intensities of the protein bands observed on the gel images, each gel was separately analyzed with DELTA 2D software. The intensity of each identified spot was computed, normalized and comparative plots for HSA, HIgG, and HFib are presented in Fig. 3, respectively. The relative abundance of the surface adsorbed HSA, HIgG (light and heavy chain), HFib (alpha, beta and gamma chain) for all surfaces are represented in Fig. 3. Figure 3 showed the maximum intensity of HSA (18.925 ± 3.198) from human serum adsorbed on LP1 compared to LP2 (7.041 ± 0.258), SCL (2.272 ± 0.005), and C (5.722 ± 0.220). The relative amount of IgG bound to the LP1 surfaces was much less compared to other

Table 3 Estimation of surface density (μg/cm^2) of adsorbed proteins

Surface	by BCA assay	by ELISA		
	Single component (HSA) (μg/cm^2)	Human serum		
		HSA (μg/cm^2)	HIgG (μg/cm^2)	HFib (μg/cm^2)
LP1	3.981 ± 0.115	2.456 ± 0.100	0.688 ± 0.048	nd
LP2	2.024 ± 0.092	0.793 ± 0.015	0.304 ± 0.018	nd
SCL	1.045 ± 0.095	0.618 ± 0.065	0.491 ± 0.037	0.217 ± 0.015
C	0.886 ± 0.070	0.553 ± 0.028	0.302 ± 0.048	0.097 ± 0.007
Feed concentration (mg/ml)	1	4.091 ± 0.836	1.346 ± 0.265	0.295 ± 0.127

Surfaces, as indicated, were either exposed to pure HSA solution (1.0 mg/ml) or human serum, in separate experiments. Upon completion of the incubation step, surfaces were washed and surface adsorbed proteins were eluted with 1% SDS. BCA assay was used to quantify the total amount of HSA present in the eluates from surfaces exposed to pure HSA solutions. Specific ELISA assays were used to determine the concentration of HSA, HIgG, and HFib present in the eluates from surfaces exposed to human serum, and also that of the feed serum employed

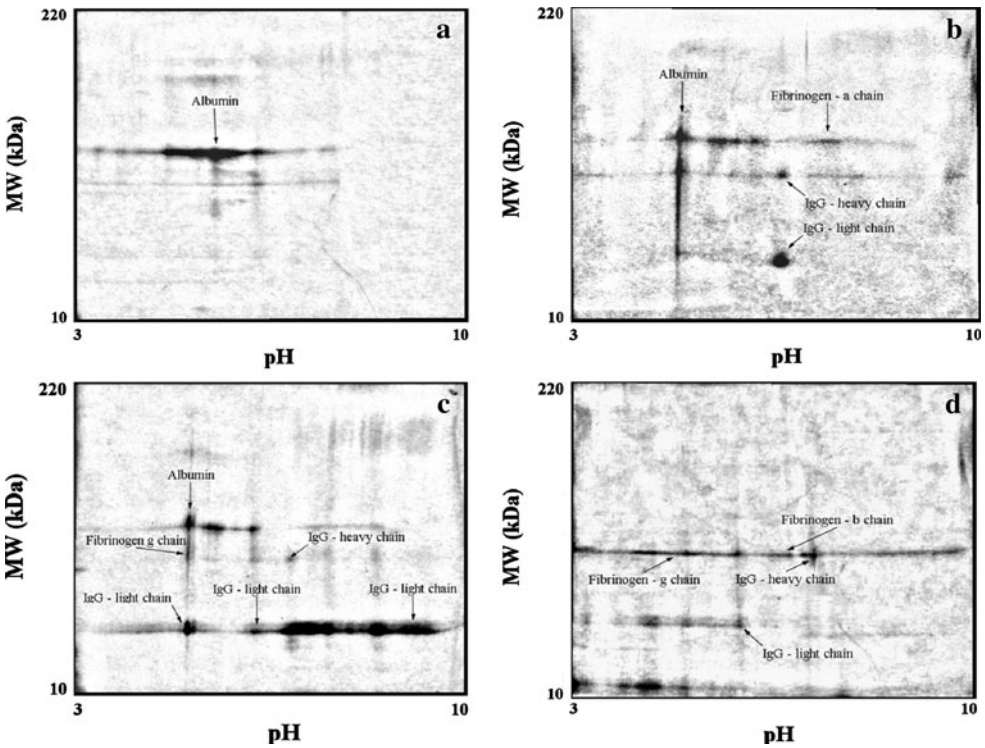

Fig. 2 *2D gel electrophoresis analysis of surface adsorbed proteins*. Surfaces were exposed to human serum for 6 h, washed and surface adsorbed proteins were eluted with 1% SDS and analyzed by 2D gel electrophoresis. (**a**) surface functionalized with LP1, (**b**) surface functionalized with LP2, (**c**) surface functionalized with SCL and (**d**) C surfaces. (a-chain: α chain, b-chain: β chain, g-chain: γ chain)

surfaces. There was a relatively large amount of light chain IgG present in the eluted protein from the SCL surface. The adsorbed HFib spots were barely detectable on LP1 and LP2 whereas they were strongly present on the SCL and C. From the gel analysis, we observed higher amounts of adsorbed HSA on surfaces derivatized with LP1 and LP2 when compared to either C or SCL-derivatized surfaces. However, to get rid of ambiguity from either an over or under estimation of silver stained gel pictures and to directly quantify the amount of specifically adsorbed proteins, the eluted fractions were analyzed by specific ELISA assays and reported (Table 3).

The abilities of the modified surfaces to bind platelets were evaluated. The number of bound platelets was measured by LDH assay and is shown in Fig. 4. Figure 4 shows the number of platelets adhered to the various surfaces (platelets/cm^2) that were directly exposed to serum. Collagen-coated glass slides were included as a positive control. A platelet density of 2.1×10^6 platelets/cm^2 was obtained for the collagen-coated surfaces. Surfaces derivatized with LP1 had the lowest platelet densities, 4.0×10^5 platelets/cm^2. The following trend was noted for platelet densities: LP1 < LP2 < SCL < C. In a separate experiment, test surfaces were pre-incubated with HSA followed

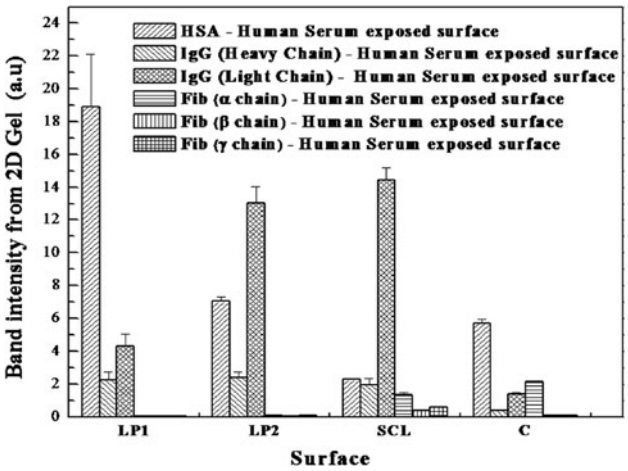

Fig. 3 2D gel images (from Fig. 2) were mapped and analyzed with Delta2D software. The area, designated for HSA, HIgG (light and heavy chain) and HFib (α, β and γ chain) were quantified and software generated averaged area $\pm$ SE ($n = 3$) is presented in the graph

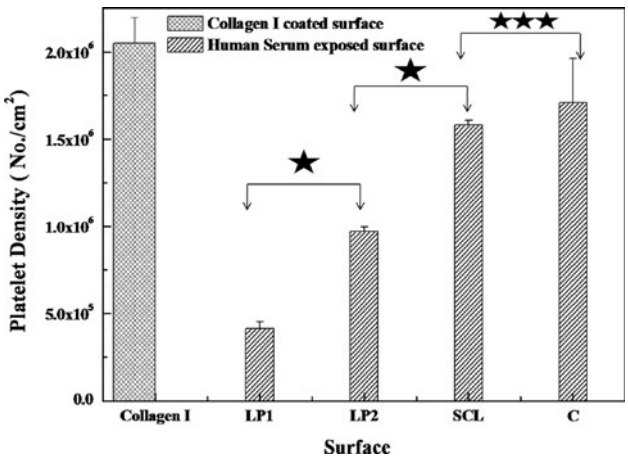

Fig. 4 Surface density (number of platelets/unit area) of adsorbed platelets by LDH assay. Surfaces, as indicated, were incubated in human serum, washed and followed by incubation with washed platelets. The results are expressed as platelet density $\pm$ SE ($n = 10$). * The amount of adhered platelets was significantly different ($P < 0.005$); *** the amount of adhered platelets was not statistically different ($P < 0.1$)

by human serum incubation. Pre-exposure with HSA on the LP1 and LP2 surface further reduced the adhesion of platelets (supplementary Figure 3). The platelet adherence on all surfaces was statistically different from the positive control ($P < 0.005$).

Figures 5 and 6 show representative SEM pictures of platelets on indicated surfaces that were first exposed to human serum followed by washed platelets. The morphology of adhered platelets was classified according to Cooper's scheme (Table 4). As shown in Fig. 5, surfaces derivatized with LP1 (a of Fig. 5) demonstrated a reduced adhesion of platelets. A higher magnification of the adhered platelets on surfaces derivatized with LP1 showed disc shaped platelets with no pseudopodia formation (b of Fig. 5). Although the platelet density of surfaces derivatized with LP2 were higher when compared to LP1 derivatized surfaces, similar morphologies were observed (c, d). In contrast, a dense adherence of platelets along with clear pseudopodia formation were observed on surfaces derivatized with SCL (a, b of Fig. 6) or C surface (c, d of Fig. 6). The dense adherence of platelets on surfaces derivatized with SCL or C is further supported by the higher values of platelet densities obtained (Fig. 4). The adhered platelets on collagen I coated surface was highly dense with distinct pseudopodia formation (supplementary Figure 4).

4 Discussion

In this study, material surfaces capable of selectively binding albumin in situ were generated by grafting albumin binding peptides and small chemical ligands with documented affinity for albumin. The surfaces prepared in this study with variable surface properties were tested for protein adsorption under static conditions. Silanized surfaces are non-fouling and can adsorb proteins; however, the pattern of adsorbed proteins was random, similar to control surfaces. Thus, unmodified surface was selected as the control. Surfaces derivatized with LP1 were shown to be highly selective and specific towards albumin over other serum proteins and the order of selectivity of the ligands used in the present study is as follows: LP1 > LP2 > SCL > C. This observed selectivity resides in the affinity character of the peptides and their presentation upon surface immobilization. The rational of the protein adsorption experiments at pH 6.2 was to create the protonated $-NH_2$ moiety on peptides and $-N(Me)_2$ on SCL thus facilitating a charge based interaction, in addition to the affinity-based interactions with albumin (IP $\sim$ 5.5) which has a net negative charge at pH 6.2. LP1 and LP2 have disassociation constants (K_D) of 0.950 and 125 μM, respectively, and the SCL was noted to have a K_D of 10 mM [19, 21]. The enhanced albumin binding affinity of LP1 (IP = 4.4) or LP2 (IP = 8.8) derivatized surfaces at the selected pH can be attributed to the affinity-binding nature of LP1 and LP2 coupled with short-range electrostatic charge repulsion arising from the surface terminal functional groups and long-ranged hydrophobic interaction aided by the long peptide chain. In contrast to LP1 derivatized surfaces, SCL derivatized surfaces bound comparable amounts of HSA as the LP2 surface with significantly higher amounts of surface adsorbed HIgG and HFib were noted. This non-discriminating nature of the SCL derivatized surface was likely due to a weak affinity of SCL (IP $\geq$ 8.0) for HSA which is based on mixed mode interactions. The

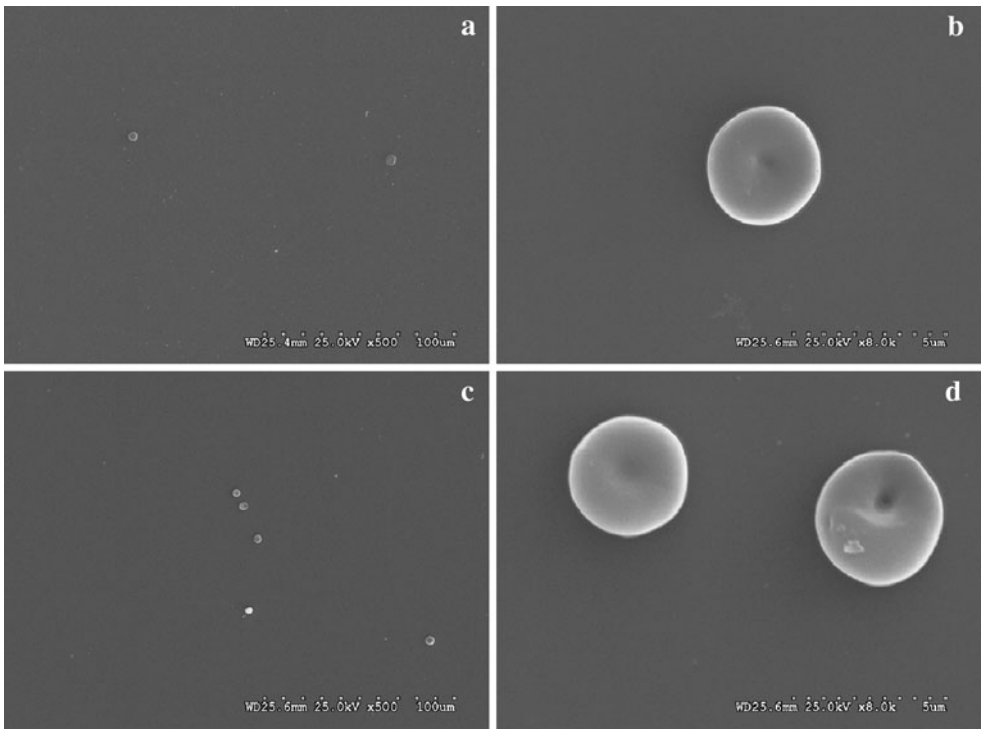

Fig. 5 *SEM micrographs of surface adhered platelets*. Surfaces, as indicated, were incubated in human serum, washed and followed by incubation with washed platelets. Surfaces were rinsed, fixed and visualized by SEM. (**a**, **b**) surface functionalized with LP1, (**c**, **d**) Surface functionalized with LP2. Scans at two different magnifications (500× and 8,000×) are shown

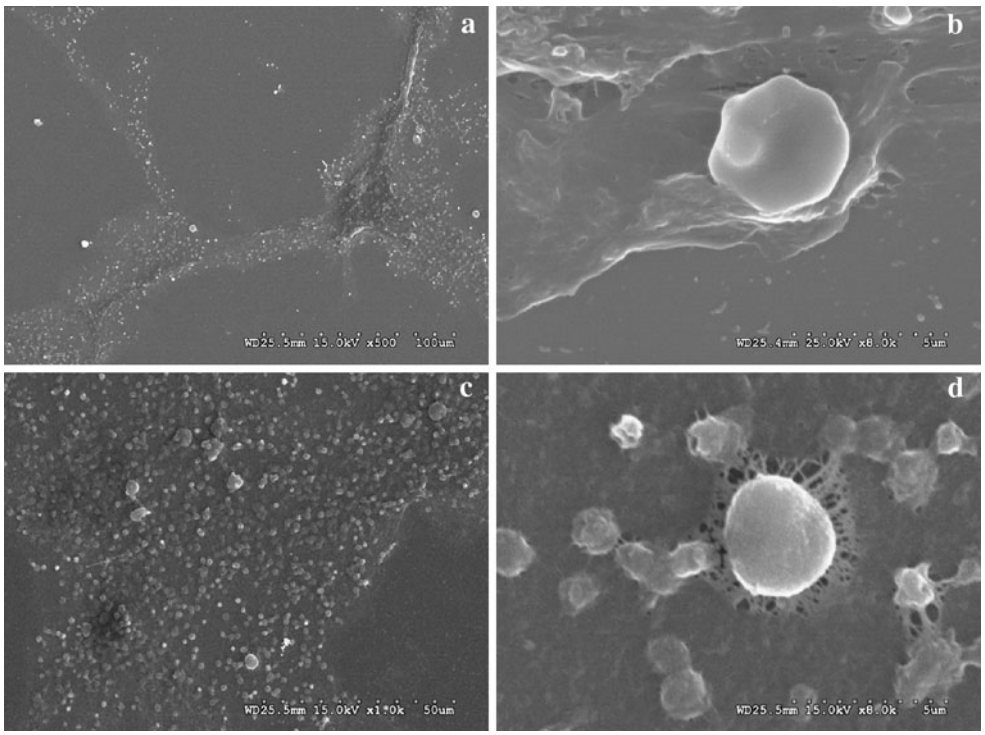

Fig. 6 *SEM micrographs of surface adhered platelets*. Surfaces, as indicated, were incubated in human serum, washed and followed by incubation with washed platelets. Surfaces were rinsed, fixed and visualized by SEM. (**a**, **b**) Surface functionalized with SCL, (**c**, **d**) unmodified control surface. Scans at two different magnifications (500× and 8,000×) are shown

Table 4 Cooper's classification of the morphology of adhered platelets

Platelet shape	Description of morphology	Surfaces
I Round	Round or disc shaped morphology and absence of pseudopodia	LP1, LP2
II Dendritic	Dendritic, rounded platelets with early pseudipodial formation	–
III Spread-dendritic	Spreading, dendritic platelets	SCL
IV Spreading	Spread platelets and their hyaloplasms with prominent pseudipodial formation	SCL and C
V Fully spread	Fully spread platelets over the entire surface	Collagen coated surface

nonspecificity of the C can be attributed to the hydrophobic nature of the C that creates a truly lipophilic based interaction aided with highly entropically driven adsorption of non-specific proteins. Similar to studies reported elsewhere, elution of bound proteins was achieved with SDS [27, 28].

A comparative analyses of the characteristics of the albumin binding surfaces previously reported in the literature reveals the following: (1) cibacron blue when immobilized on a variety of surfaces either directly or via dextran, conferred albumin binding properties with moderate specificity. Surface adsorbed HSA in the range of 0.05–2.7 μg/cm^2 was obtained depending on the polymer employed and comparable amounts of fibrinogen were also bound [13, 16, 18, 36–40]; (2) binding of C_{16}–C_{18} ligands on a variety of surfaces yielded surfaces with 0.1–2.0 μg/cm^2 of adsorbed HSA binding properties with low selectivity for HSA over other serum proteins [35, 41–44]; (3) immobilization of small ligands (e.g., 2-hydroxyethyl methacrylate, L-ascorbic acid, polylysine, etc.) on surfaces yielded surfaces that were highly non-specific and when exposed to plasma adsorbed similar amount of HSA and HFib [45–47]. Our results indicate that the linear peptide, LP1, when linked to silicon surface bound HSA over other serum proteins in a specific and a selective manner and have reduced affinity for HIgG and negligible affinity for HFib under static condition.

Previous research has identified surfaces that bind high levels of HIgG and HFib as preferred substrates for platelet adhesion and activation [1, 5, 48]. Albumin binding has been noted to preserve the nature of the surfaces as platelets have no known receptor for albumin [13, 16, 17]. Thus, as expected, surfaces derivatized with LP1 had the lowest platelet densities and rounded platelet morphology was preserved on the LP1 surfaces. The ratio of adsorbed HSA to adsorbed HIgG and HFib ($HSA/[HIgG] + [HFib]$) was around 3.0 for surfaces derivatized with LP1. The ratio of adsorbed HSA to adsorbed HIgG and HFib was around 1.0 for surfaces derivatized with SCL or C and these surfaces were noted to possess higher platelet densities with extensive spreading. Interestingly, a very low amount of surface adsorbed fibrinogen ($\sim$5 ng/cm^2) has been reported to induce maximum platelet adherence (49].

Similar to C surfaces used in this study, when silicon-alloyed pyrolytic carbon (PYC) surfaces were exposed to platelets, platelet densities in the range of 1.5–2.0 $\times$ 10^6 platelets/cm^2 were noted and dendritic to spread morphologies were observed [50]. The blood compatibility of PYC has been largely ascribed to its ability to tenaciously adsorb plasma albumin, which in turn inhibits platelet adhesion, spreading, and activation. Several investigations indicate that this mechanism may be incomplete since PYC induces extensive in vitro platelet adhesion and spreading even in the presence of albumin, and is not passive to platelet adhesion in vivo, at least as demonstrated in a non-anticoagulated sheep model [50]. Perhaps a surface modification of silicon-alloyed PYC, using a strategy similar to that proposed in this study would be successful in generating surfaces with acceptable surface properties. The surface modifications described in this study using linear peptides that bind HSA can be used to modify biomaterial surfaces owing to their selective and specific HSA binding properties.

5 Conclusion

The highlights of our present study are as follows: (1) a surface modification technique was developed to immobilize HSA-binding linear peptides and small chemical ligands on material surfaces, (2) peptide-derivatized surfaces conferred HSA-binding selectivity and specificity over other plasma proteins, (3) peptide-derivatized surfaces were shown to possess the lowest platelet adherence, and (4) rounded morphology of the platelets was preserved on peptide-derivatized surfaces. Our current studies include the evaluation of these surfaces under shear flow in a flow chamber when using platelet poor plasma and the quantification of coagulation parameters.

Acknowledgments This work was partially supported by NSF Grant CTS-0411632 and Army Research Laboratory W911NF-04-2-0011. We are thankful to Gaye Homer, University of Nebraska Health Center, Lincoln, NE for letting us use the platelet counting instrument; Dr. H. Chen and Dr. Y. Joe. Zhou of microscopy facility of Center of Biotechnology; Dr. D. W. Thompson and Dr. T. Hofmann of Center for Materials Research and Analysis, University of

Nebraska, Lincoln, NE for in hand training at SEM and Ellipsometry facility, respectively.

References

1. Tang L, Eaton JW. Fibrin(ogen) mediates acute inflammatory responses to biomaterials. J Exp Med. 1993;178:2147–56.
2. Gorbet MB, Sefton MV. Biomaterial-associated thrombosis: roles of coagulation factors, complement, platelets and leukocytes. Biomaterials. 2004;25(26):5681–703.
3. Ratner BD. Blood compatibility: a perspective. J Biomater Sci Polymer Edn. 2000;11(11):1107–19.
4. Castner DG, Ratner BD. Biomedical surface science: Foundations to frontiers. Surf Sci. 2002;500:28–60.
5. Vroman L. What factors determine thrombogenicity. Bull N Y Acad Med. 1972;48(2):302–10.
6. Brash JL. Protein interactions with solid surfaces following contact with plasma and blood. Makromol Chem Macromol Symp. 1988;17:441–52.
7. Anderson JM, Bonfield TL, Ziats NP. Protein adsorption and cellular adhesion and activation on biomedical polymers. Int J Artif Organ. 1990;13(6):375–82.
8. Lyman DJ, Baszkin A. The interaction of plasma proteins with polymers I. Relationship between polymer surface energy and protein adsorption/desorption. J Biomed Mater Res. 1980;14(4): 393–403.
9. Lyman, DJ, Brash, JL, Adsorption of plasma proteins in solution to uncharged, hydrophobic polymer surfaces. J Biomed Mater Res 1969;3(1) 175–189.
10. Lyman DJ, Kim SW. Interface reactions between artificial membranes and blood. Adv Nephrol Necker Hosp. 1972;2:97–107.
11. Lyman DJ, Metcalf LC, Albo D, Richards KF, Lamb J. The effect of chemical structure and surface properties of synthetic polymers on the coagulation of blood. III. *In vivo* adsorption of proteins on polymer surfaces. Trans Am Soc Artif Intern Organs. 1974;20(B): 474–8.
12. Mustard JF, Packham MA. Factors influencing platelet function: adhesion, release and aggregation. Pharmacol Rev. 1970;22: 97–187.
13. Keogh JR, Eaton JW. Albumin binding surfaces for biomaterials. J Lab Clin Med. 1994;121:537–45.
14. McFarland CD, De Filippis C, Jenkins M, Tunstell A, Rhodes NP, Williams DF, Steele JG. Albumin-binding surfaces: in vitro activity. J Biomater Sci Polymer Edn. 1998;9(11):1227–39.
15. Kao WJ, Sapatnekar S, Hiltner A, Anderson JM. Complement-mediated leukocyte adhesion on poly(etherurethane ureas) under shear stress in vitro. J Biomed Mater Res. 1996;32:99–109.
16. Keogh JR, Eaton JW. Albumin affinity biomaterial surfaces. Cells Mater. 1996;6(1–3):209–20.
17. Keogh JR, Velander FF, Eaton JW. Albumin-binding surfaces for implantable devices. J Biomed Mater Res. 1992;26(4):441–56.
18. Martins MCL, Naeemi E, Ratner BD, Barbosa MA. Albumin adsorption on Cibacron Blue F3G-A immobilized onto oligo(ethylene glycol)-terminated self-assembled monolayers. J Mater Sci: Mater Med. 2003;14(11):945–54.
19. Sato AK, Sexton DJ, Morganelli LA, Cohen EH, Wu QL, Conley GP, Streltsova Z, Lee SW, Devlin M, De Oliveira DB, Enright J, Kent RB, Wescott CR, Ransohoff TC, Ley AC, Ladner RC. Development of mammalian serum albumin affinity purification media by peptide phage display. Biotechnol Prog. 2002; 18(2):182–92.
20. Desai NP, Hubbell JA. Biological responses to polyethylene oxide modified polyethylene terephthalate surfaces. J Biomed Mater Res. 1991;25(7):829–43.
21. Subramanian A, Rau AV, Kaligotla H. Surface modification of chitosan for selective surface-protein interaction. Carbohydr Polym. 2006;66(3):321–32.
22. GuhaThakurta S, Subramanian A. Effect of hydrofluoric acid in oxidizing acid mixtures on the hydroxylation of silicon surface. J Electrochem Soc. 2007;154(11):136–46.
23. Guha Thakurta S. Design, development of *in situ* albumin binding surfaces. Evaluation in the paradigm of blood-biomaterial compatibility. Lincoln: University of Nebraska Lincoln; 2009.
24. Gandara JS, Mahia PL, Losada PP, Lozano JS, Abuin SP. Overall migration and specific migration of bisphenol A diglycidyl ether monomer and m-xylylenediamine hardener from an optimized epoxy-amine formulation into water-based food simulants. Food Addit Contam. 1993;10(5):555–65.
25. Van Oss CJ. Interfacial forces in aqueous media. New York: Marcel Dekker; 1969.
26. van Oss CJCMK, Good RJ. Monopolar surfaces. Adv Colloid Interface Sci. 1987;28:35–64.
27. Magnani A, Barbucci R, Lamponi S, Chiumento A, Paffetti A, Trabalzini L, Martelli P, Santucci A. Two-step elution of human serum proteins from different glass-modified bioactive surfaces: a comparative proteomic analysis of adsorption patterns. Electrophoresis. 2004;25(14):2413–24.
28. Cornelius RM, Archambault Jacques G, Chan BerryLeslie, Anthony KC, Brash John L. Adsorption of proteins from infant and adult plasma to biomaterial surfaces. J Biomed Mater Res A. 2001;60(4):622–32.
29. Subramanian A, Van Cott KE, Milbrath DS, Velander WH. Role of local antibody density effects on immunosorbent efficiency. J Chromatogr A. 1994;672(1–2):11–24.
30. Subramanian A, Butler SP, Gwazdauskas FC, Lubon H, Velander WH. Expression of human fibrinogen in transgenic mice. In: Bumgardner JD, Puckett AD, editors. Southern Biomedical Engineering Conference. Institute of Electrical and Electronics Engineers. Apr. 4–6, Mississippi: Biloxi; 1997. p. 57–60.
31. Taoa W, Zhoub H, Zhanga Y, Lia G. Novel silsesquioxane mixture-modified high elongation polyurethane with reduced platelet adhesion. Appl Surf Sci. 2008;254(9):2831–6.
32. Chiumiento A, Lamponi S, Barbucci R. Role of fibrinogen conformation in platelet activation. Biomacromolecules. 2007;8(2): 523–31.
33. Wu YZ, Meyerhoff ME. In vitro platelet adhesion on polymeric surfaces with varying fluxes of continuous nitric oxide release. J Biomed Mater Res A. 2007;81:956–63.
34. Wu YSFI, Ratner BD, Horbett TA. The role of adsorbed fibrinogen in platelet adhesion to polyurethane surfaces: a comparison of surface hydrophobicity, protein adsorption, monoclonal antibody binding, and platelet adhesion. J Biomed Mater Res A. 2005;74(4):238–722.
35. Frautschi JR, Eberhart RC, Hubbell JA. Alkylated cellulosic membranes with enhanced albumin affinity: influence of competing proteins. J Biomater Sci Polymer Edn. 1995;7(7):563–75.
36. Demiryas N, Tuzmen N, Galaev IY, Piskin E, Denizli A. Poly(acrylamide-allyl glycidyl ether) cryogel as a novel stationary phase in dye-affinity chromatography. J Appl Polym Sci. 2007;105(4):1808–16.
37. Ma ZY, Guan YP, Liu HZ. Affinity adsorption of albumin on Cibacron Blue F3GA-coupled non-porous micrometer-sized magnetic polymer microspheres. React Funct Polym. 2006;66(6): 618–24.
38. Odabasi M, Denizli A. Cibacron Blue F3GA incorporated magnetic poly(2-hydroxyethyl methacrylate) beads for lysozyme adsorption. J Appl Polym Sci. 2004;93(2):719–25.
39. Martins MCL, Ratner BD, Barbosa MA. Protein adsorption on mixtures of hydroxyl- and methyl-terminated alkanethiols self-

assembled monolayers. J Biomed Mater Res A. 2003;67A(1): 158–71.
40. Wang D, Chen B, Ji J, Feng L. Selective adsorption of serum albumin on biomedical polyurethanes modified by a poly(ethylene oxide) coupling-polymer with cibacron blue (F3G-A) end groups. Bioconj Chem. 2002;13(4):792–803.
41. Goncalves IC, Martins MCL, Barbosa MA, Naeemi E, Ratner BD. Selective protein adsorption modulates platelet adhesion and activation to oligo(ethylene glycol)-terminated self-assembled monolayers with C18 ligands. J Biomed Mater Res A. 2009; 89A(3):642–53.
42. Goncalves IC, Martins MCL, Barbosa MA, Ratner BD. Protein adsorption on 18-alkyl chains immobilized on hydroxyl-terminated self-assembled monolayers. Biomaterials. 2005;26(18): 3891–9.
43. Wang DA, Ji J, Feng LX. Selective binding of albumin on stearyl poly(ethylene oxide) coupling polymer-modified poly(ether urethane) surfaces. J Biomater Sci Polymer Edn. 2001;12(10): 1123–46.
44. Riccitelli SD, Schlatterer RG, Hendrix JA, Williams GB, Eberhart RC. Albumin coatings resistant to shear-induced desorption. Trans Am Soc Artif Intern Organs. 1985;31:250–6.
45. Chandy T, Sharma CP. Changes in protein adsorption on polycarbonate due to L-ascorbic acid. Biomaterials. 1985;6(6): 416–20.
46. Chandy T, Sharma CP. Polylysine-immobilized chitosan beads as adsorbents for bilirubin. Artif Organs. 1992;16(6):568–76.
47. Sharma CP, Jayasree G, Najeeb PP. Introduction of surface functional groups onto biomaterials by glow discharges. J Biomater Appl. 1987;2(2):205–18.
48. Tang L, Ugarova TP, Plow EF, Eaton JW. Molecular determinant of acute inflammatory responses to biomaterials. J Clin Invest. 1996;97(5):1329–34.
49. Cao L, Sukavaneshvar S, Ratner BD, Horbett TA. Glow discharge plasma treatment of polyethylene tubing with tetraglyme results in ultralow fibrinogen adsorption and greatly reduced platelet adhesion. J Biomed Mater Res A. 2006;79A(4):788–803.
50. Goodman SL, Tweden KS, Albrecht RM. Platelet interaction with pyrolytic carbon heart-valve leaflets. J Biomed Mater Res. 1996;32(2):249–58.